Chapter 2

Statistical Physics of Stiff Biopolymers

2.1 Introduction

In recent years, statistical mechanics of semiflexible polymers has emerged as an active area of research. This has been triggered by single molecule experiments designed to understand the role of elasticity of these polymers. Elastic properties of polymers are of importance in biology as in the structure of the cytoskeleton, a biopolymer network which controls cell mechanics [1, 2]. The parameter which determines the stiffness of a polymer is β, the ratio of its contour length L to the persistence length L_P. While the entire range of β is of biological interest, in this chapter we focus attention on rigid filaments such as actin filaments and microtubules which constitute the cytoskeletal structure and serve as tracks for motor proteins like myosin and kinesin[2, 3]. Recently, filaments of intermediate rigidity like neurofilaments have also been studied in some detail[4]. It has been shown that some remarkable features of single stiff filament bending response are relevant to crosslinked biofilament networks [2]. A good understanding of the elastic properties of biopolymers at the single molecule level, is essential to a study of polymer networks.

There are two classes of experiments which probe the elasticity of single biopolymers. In one class of experiments[5] a semiflexible polymer molecule is pulled and stretched to study its"equation of state" by measuring its extension as a function of applied force. In the other class of experiments, one tags the ends with fluorescent dye[6, 7] to determine the distribution of end-to-end distances. Such experimental studies provide valuable insight into

the mechanical properties of semiflexible polymers. A good theoretical model is needed to correctly interpret these experiments. A simple and popular model which captures much of the physics is the Worm Like Chain model[8].

In this chapter we first analyze the bending degrees of freedom of a stiff polymer where at least one end of the polymer is *clamped*. By this it is meant that the tangent vector at this end is kept in a fixed direction. The tangent vector of a stiff polymer executes small wanderings around this fixed direction. The theoretical analysis for the statistical mechanics of a stiff polymer, clamped at least at one end is similar to that of a polymer in the high stretch limit. We refer to this approximation as the paraxial approximation. This approximation has been previously used to study the elasticity of twist storing flexible stretched polymers[9, 10, 11, 12] in the paraxial worm like chain model (PWLC model). In reference [13] an "exact" numerical scheme had been used for a semiflexible polymer with free boundary conditions for the end tangent vectors. The main difference in the numerical scheme presented here is that we impose boundary conditions on the tangent vectors at the ends. As a general rule, in the stiff regime the convergence of the numerical scheme is poorer and therefore one needs to use larger matrix sizes. The search for simple analytic forms to describe the elastic properties of stiff polymers is therefore well motivated. Subsequently we extend the above model to capture the essential features of twist elasticity as well. Twist elasticity of biopolymers has important relevance to biological processes;for example DNA-histone association which makes use of DNA supercoiling. One can experimentally study the response of a semiflexible polymer molecule to forces and torques by measuring its extension as a function of applied forces and torques[5].

For stiff polymers, the experimentally measured mean values crucially depend [14] on the precise choice of the ensemble. This is due to finite size fluctuation effects, which are entirely absent in the elasticity of a classical rod. For instance, one gets qualitatively distinct features in force-extension curves depending on whether the force or the extension is held constant in an experimental setup [15, 16, 17]. This is an aspect of stiff polymer statistical mechanics which is both theoretically challenging and experimentally significant. In this

chapter, we remain throughout in the constant force and constant torque ensemble measure the mean extension and mean link.

The organization of this chapter is as follows. We first present results based on an "exact" numerical scheme for stiff polymers for two different boundary conditions, one in which both ends are clamped and the other in which one end is clamped and the other end is free. We then present simple analytical forms for these two cases. This is followed by a discussion of the buckling of stiff polymers and the consequent breakdown of the paraxial approximation. Next we extend the pure bend model to include the twist degrees of freedom and derive an analytical expression for the writhe distribution. We discuss the buckling of stiff polymers under applied torques and then derive simple analytical expressions for the torque-link relation.

2.2 The Exact Numerical Scheme

Our starting point is the *Worm Like Chain (WLC) model* in which the configuration C of the polymer is described by a space curve $\vec{x}(s)$, with s the arc-length parameter ($0 \leq s \leq L$) ranging from 0 to L, the contour length of the polymer. The tangent vector $\hat{t} = d\vec{x}/ds$ to the curve is a unit vector

$$\hat{t}.\hat{t} = 1 \tag{2.1}$$

and the curvature of the polymer is given by $\kappa = |d\hat{t}/ds|$.

One can study the case of stiff polymers using a combination of analytical and numerical techniques [13]. Let one end of the polymer be fixed at the origin and a stretching force F be applied in the $\hat{z}$ direction, which we refer to as the north pole of the sphere of directions. Introducing a dimensionless force variable $f = \frac{FL_p}{k_BT}$, where k_BT is the thermal energy we can express the partition function $Z(f)$ as

$$Z(f) = \mathcal{N} \int \mathcal{D}[\hat{t}(\tau)] e^{-\int_0^\beta d\tau [1/2(d\hat{t}/d\tau)^2 - f\hat{t}_z]} \tag{2.2}$$

where $\beta = L/L_p$. Eq. (2.2) can be interpreted as the path integral representation for the kernel of a *quantum* particle on the surface of a sphere at inverse temperature β. Thus we

can express $Z(f)$ as the quantum amplitude to go from an initial tangent vector $\hat{t}_A$ to a final tangent vector $\hat{t}_B$ in imaginary time β in the presence of an external potential $-f\cos\theta$:

$$Z(f,\hat{t}_A,\hat{t}_B) =< \hat{t}_A|\exp[-\beta\hat{H}_f]|\hat{t}_B > \tag{2.3}$$

The Hamiltonian $\hat{H}_f = -\frac{\nabla^2}{2} - f\cos\theta$ is that of a rigid rotor[18] in a potential. In the absence of a force, the free Hamiltonian is $H_0 = -\frac{1}{2}\nabla^2$. By choosing a standard basis in which H_0 is diagonal we find that H is a symmetric tridiagonal matrix with diagonal elements $H_{l,l} = l(l+1)/2$ and superdiagonal elements $H_{l,l+1} = f(l+1)\sqrt{1/((2l+1)(2l+3))}$. Inserting a complete set of eigenstates of the free Hamiltonian into Eq. (2.3), we find $Z(f,\hat{t}_A,\hat{t}_B) =$

$$\sum_{m,n} < \hat{t}_A|\psi_n >< \psi_n|\exp[-\beta\hat{H}_f]|\psi_m >< \psi_m|\hat{t}_B > \tag{2.4}$$

where $\hat{M}^f = \exp[-\beta\hat{H}_f]$. From this general form, we can compute the partition function in the present cases of interest.

In Ref. [13] the elastic properties of polymers with free boundary conditions had been studied: the directions of the tangent vectors at both ends were integrated over. In the present study, we will fix the tangent vector at the ends (one or both) to lie along the $\hat{z}$ direction. To implement this numerically, we have to evaluate the eigenfunctions in Eq. (2.4) at this value of $\hat{t}$.

(i)*both ends clamped*: $\hat{t}_A = \hat{t}_B = \hat{z}$. While a complete set of eigenstates are labelled by (l,m), only the $m = 0$ terms contribute here because of azimuthal symmetry and we have

$$Z(f,\hat{z},\hat{z}) = \sum_{l,l'} U_l M^f_{l,l'} U_{l'} = U.M.U \tag{2.5}$$

where $U_l = \sqrt{\frac{2l+1}{4\pi}}$.

(ii)*one end clamped*: Integrating Eq. (2.4) over $\hat{t}_B$, we find that

$$Z(f,\hat{t}_A) = \sum_{l} U_l M^f_{l0} = (U.M^f)_0 \tag{2.6}$$

Both Eqs. (2.5) and (2.6) are suitable for numerical implementation. H_f is an infinite symmetric matrix. We truncate it to finite order N and choose N large enough to attain the desired accuracy [19].

While this numerical method is effective, it has a limitation in describing stiff polymers due to the poor convergence of statistical sums in Eq. (2.4). For stiff polymers a convenient and accurate analytical approximation scheme can be developed as shown below.

2.3 Analytical Results

For a stiff polymer with one end clamped along the $\hat{z}$ direction, we can approximate the sphere of directions by a tangent plane at the north pole of the sphere as the angular coordinate θ always remains small. Introducing Cartesian coordinates $\xi_1 = \theta\cos\phi$ and $\xi_2 = \theta\sin\phi$ on the tangent plane R^2 at the north pole one can express the small θ Hamiltonian H as $H = H_P - f$ where H_P is

$$H_P = \frac{1}{2}{p_{\xi_1}}^2 + \frac{1}{2}{p_{\xi_2}}^2 + \frac{f}{2}({\xi_1}^2 + {\xi_2}^2); \tag{2.7}$$

We notice that H_P is the Hamiltonian of a two-dimensional harmonic oscillator with a frequency $\omega = \sqrt{f}$. For a single oscillator in real time the propagator is given by[20]: $K(\xi_i, \xi_f, T) =$

$$F(T)\exp\frac{i\omega}{2\sin\omega T}[(\xi_i^2 + \xi_f^2)\cos\omega T - 2\xi_i\xi_f] \tag{2.8}$$

where $F(T) = \sqrt{\frac{\omega}{2\pi i\sin(\omega T)}}$.

Case (i): both end tangent vectors clamped along the $\hat{z}$-direction: Setting $\xi_i = \xi_f = 0$ in Eq. (2.8) and continuing the expression to imaginary time results in the trigonometric functions being replaced by hyperbolic ones. We can express the partition function $Z(f)$ as $\exp(\beta f)$ times the product of the propagators of two independent harmonic oscillators:

$$Z(f) = \sqrt{f}\exp(\beta f)/(2\pi\sinh(\beta\sqrt{f})). \tag{2.9}$$

in Euclidean time β; the free energy is $G(f) = -\log Z(f)/\beta$

$$= [\frac{-1}{2\beta}logf - f + \frac{1}{\beta}log(2\pi) + \frac{1}{\beta}log[\sinh(\beta\sqrt{f})] \tag{2.10}$$

The mean extension $<\zeta> = <z>/L = -\partial G(f)/\partial f$ is given by (See Fig. 2.1).

$$<\zeta> = 1 + 1/(2\beta f) - \coth(\beta\sqrt{f})/(2\sqrt{f}). \tag{2.11}$$

where $< \zeta >$ is the $\hat{z}$ component of the extension (or the end-to-end distance vector). Note in Fig.(2.1) that the analytical form agrees with the numerical scheme to an accuracy of about 1%.

Case (ii): A stiff polymer with one end tangent vector pointing along the $\hat{z}$-direction and the other end free:

In this case the propagator for the harmonic oscillator has to be integrated over the final coordinates ξ_f and evaluated at $\xi_i = 0$. The partition function in this case turns out to be

$$Z(f) = \exp(\beta f)/\cosh(\beta\sqrt{f}). \tag{2.12}$$

From the expression of the partition function, we get the free energy

$$G(f) = -f + \frac{1}{\beta} log[\cosh(\beta\sqrt{f})] \tag{2.13}$$

and differentiate it with respect to f to get the force - extension relation -

$$< \zeta >= 1 - \tanh(\beta\sqrt{f})/(2\sqrt{f}). \tag{2.14}$$

Note that even at zero force, there is a nonzero extension, because of the boundary condition and the stiffness of the polymer. Fig.(2.2) shows a comparison of the force extension curves for the two boundary conditions. We find, as expected, that for the same force, the extension is larger for the more constrained boundary condition [Case(i)] compared to a less constrained one [Case(ii)]. For positive forces the paraxial approximation is very good and the forms are displayed in Eqs. (2.11) and (2.14). For large positive forces they become $< \zeta >= 1 - \frac{1}{2\sqrt{f}}$ [13, 18] as expected.

2.4 Force induced buckling

For negative forces, the hyperbolic functions appearing in Eqs. (2.9) and (2.12) go over to circular functions. For instance, for the case in which both end tangent vectors are clamped along the $\hat{z}$ direction, for negative f, our simple analytical form for the partition function reads

$$Z(f) = \frac{\sqrt{-f}e^{\beta f}}{2\pi\sin(\beta\sqrt{-f})} \tag{2.15}$$

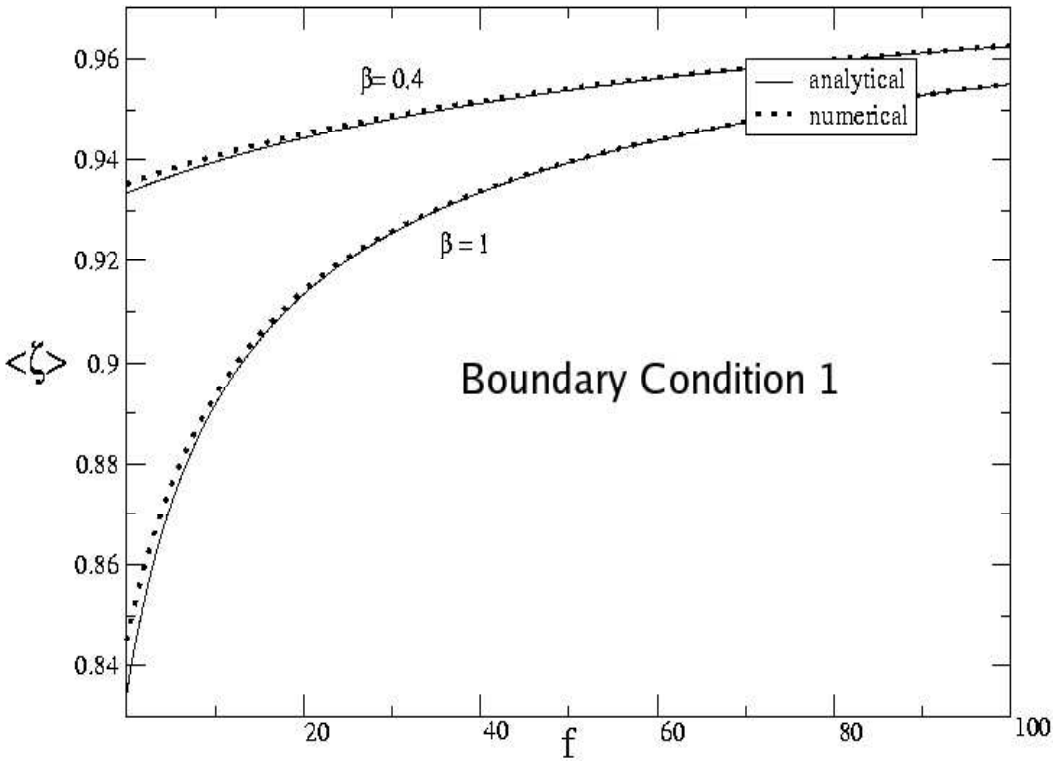

Figure 2.1: The mean extension is plotted against the force f for $\beta = .4, 1$ for a setup with both ends clamped.

and varies continuously with f as f ranges from positive to negative values. As the compressive force is increased, we find that at a critical value of the force f the extension $< \zeta >$ spontaneously decreases. This is the analogue here of the classical Euler buckling instability which occurs for rods.

Consider the mean extension versus force relation [Eq.(2.11)] for negative forces (i.e. for compressive forces). For negative values of forces Eq.(2.11) reduces to

$$< \zeta >= 1 + 1/(2\beta f) - \cot(\beta \sqrt{-f})/(2 \sqrt{-f}). \tag{2.16}$$

which can be rewritten in the form

$$< \zeta >= 1 + \beta u(x). \tag{2.17}$$

where $x = \beta \sqrt{-f}$ and

$$u(x) = \frac{\cot(x)}{2x} - \frac{1}{2x^2}$$

The criterion for the onset of the buckling instability is the divergence of $\partial < \zeta > /\partial f$.

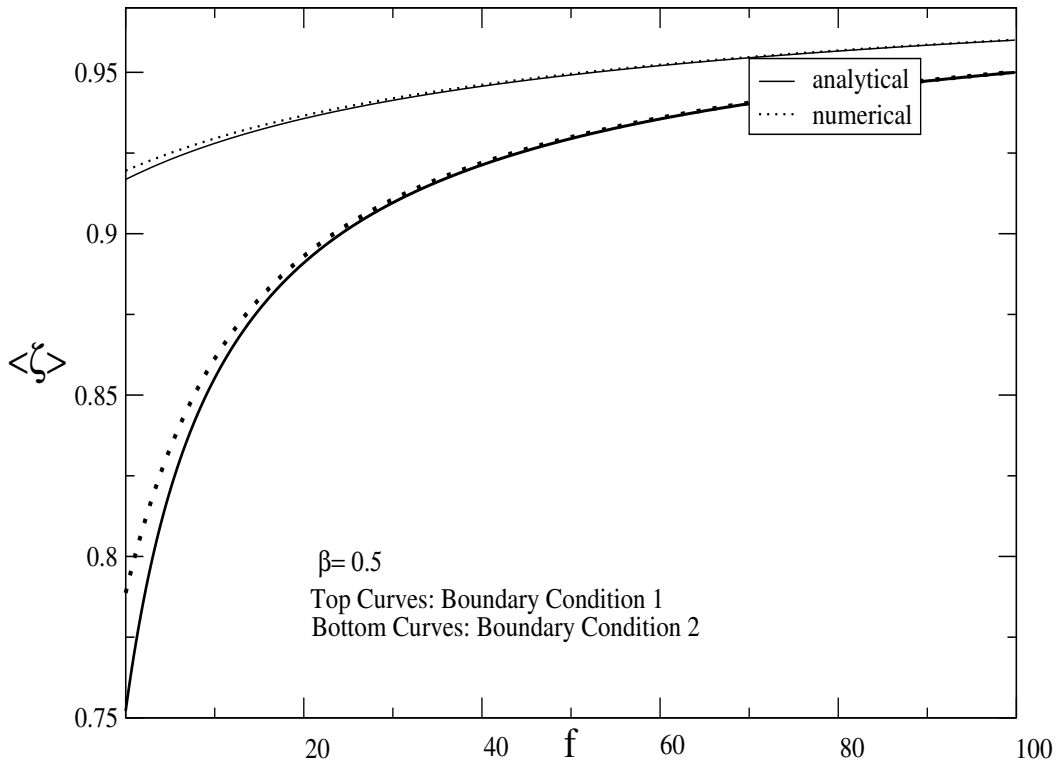

Figure 2.2: The figure demonstrates that force-extension relations depend on the boundary conditions. Note that as expected, for a given force, the extension is greater for the case where *both* ends are clamped in the $\hat{z}$ direction.

From Eq.(2.17) this is equivalent to the divergence of $\partial u/\partial x$, which takes place at a value of $x_c = \pi$. This gives us the following expression for the critical force for buckling[21]:

$$f_c = -\left(\frac{\pi}{\beta}\right)^2$$

Because of the quadratic dependence, the compressive force needed to buckle a polymer rises sharply with stiffness. The mean extension versus force curves displayed in Fig.(2.3) demonstrate the phenomenon of buckling. As expected, we notice that as β goes up, the magnitude of the critical force f_c needed to buckle the polymer goes down.

A stiff polymer is energy dominated and its buckling is very similar to that of a classical rod subject to identical boundary conditions and a compressive force. The effect of thermal fluctuations is to slightly "round off" the transition from the straight to the buckled configuration. This is due to thermally activated processes that permit the polymer to overcome the elastic energy barrier. As a result the buckling force for a stiff polymer is slightly smaller in

magnitude than the f_c given above.

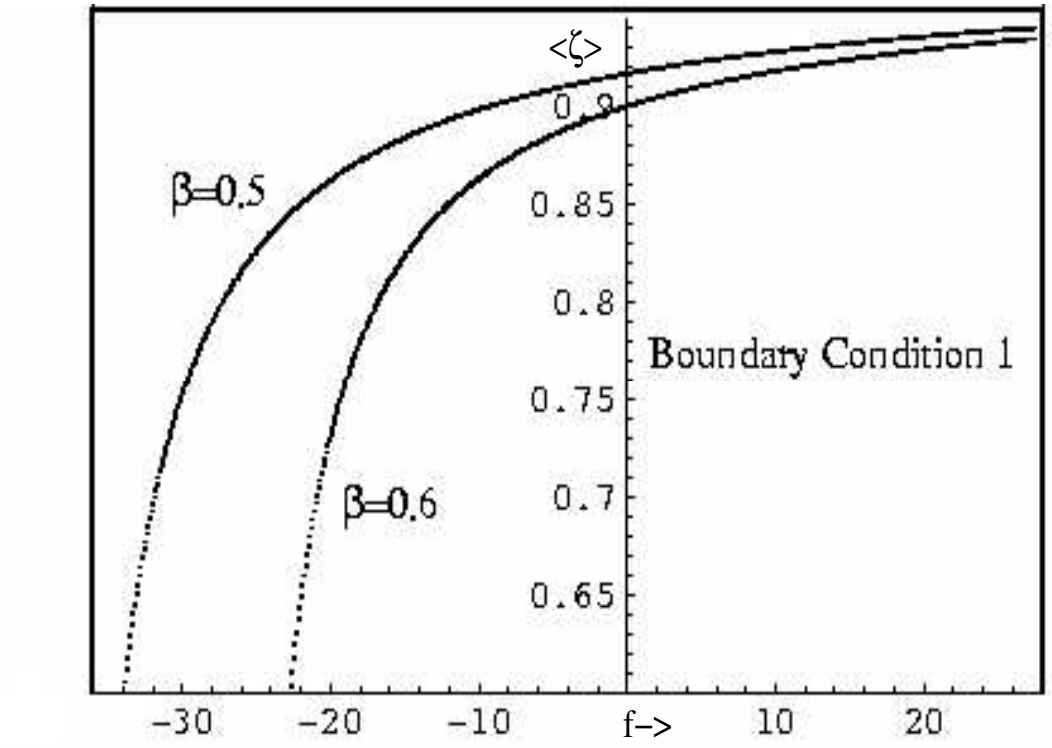

Figure 2.3: Figure shows buckling *i.e.* spontaneous decrease in extension under a compressive force for a stiff polymer with end tangent vectors clamped for $\beta = .5$ and $\beta = .6$. Note that buckling takes place at a smaller magnitude of the compressive force f for a larger β.

2.5 Stiff Polymers with Twist Degrees of Freedom

So far in this chapter we have discussed the pure bend model of the elasticity properties of stiff polymers[22]; now we extend the above model to capture the essential features of twist elasticity as well. Twist elasticity of biopolymers has important relevance to biological processes;for example packaging of DNA in a cell nucleus a few microns across involves DNA-histone association which makes use of DNA supercoiling.

We derive a simple analytical expression for the writhe distribution at zero forces. We study the elastic response of a stiff polymer to forces and torques applied at one of its ends and discuss the buckling of stiff polymers under applied torques. We also derive simple analytical expressions for the torque-twist relations. We consider boundary conditions in

which both the ends of the polymer are *clamped*. The tangent vector at the clamped ends are kept fixed in the z - direction.

2.6 The partition function

Our starting point is the Worm Like Chain (*WLC*) model with both bend and twist degrees of freedom. In this model, the polymer is modelled as a framed space curve $C = \{\vec{x}(s), \hat{e}_i(s)\}, i = 1, 2, 3$, where $0 \leq s \leq L$ is the arclength parameter along the curve. The unit tangent vector $\hat{e}_3 = d\vec{x}/ds$ to the curve describes the bending of the polymer while the twisting is captured by a unit vector $\hat{e}_1$ normal to $\hat{e}_3$; $\hat{e}_2$ is then fixed by $\hat{e}_2 = \hat{e}_3 \times \hat{e}_1$ to complete the right handed moving frame $\hat{e}_i(s), i = 1, 2, 3$. The energy $\mathcal{E}[C]$ of a configuration of the polymer is a sum of contributions coming from its bending and twisting modes. For a stiff polymer with one end clamped along the $\hat{z}$ direction, we can approximate the sphere of directions by a tangent plane at the north pole of the sphere as the angular coordinate θ always remains small. In this limit where the tangent vector never wanders too far away from the north pole of the sphere of directions, the polymer Hamiltonian[9, 10, 11, 23, 24] reduces to :

$$H_{PWLC} = \frac{p_\theta^2}{2} + \frac{(p_\phi - A_\phi)^2}{2\theta^2} + \frac{B^2\alpha}{2} - f(1 - \frac{\theta^2}{2})$$

which can be written as

$$H_{PWLC} = H_P - f + \frac{B^2\alpha}{2}$$

where H_P is the Hamiltonian of interest in the paraxial limit after we take out a constant piece; $\alpha = L_{BP}/L_{TP}$ where L_{BP} is the bend persistence length and L_{TP} is the the twist persistence length. Without loss of generality, we can set $\alpha = 0$ (see below) and we consider twist to be infinitely expensive energetically and all of the link resulting from the applied torque goes into the writhe. The constant B corresponds to the conserved momentum conjugate to the Euler angle ψ. It is related to the applied torque through the relation $B^2 = -\tau^2$ [11] where τ has the interpretation of the applied torque. We introduce a dimensionless force variable $f = FL_{BP}/k_BT$ where F is the stretching force and k_BT is the thermal energy. The 'vector potential' $A_\phi = B\frac{\theta^2}{2}$. Thus the PWLC maps onto the problem of a particle moving on a plane

in the presence of a magnetic field B and an oscillator confining potential which stems from the small θ approximation $-f\cos\theta \approx -f(1-\frac{\theta^2}{2}) = -f + f\frac{\theta^2}{2}$[9, 10]. Notice that in the stiff limit ($\beta \sim 1$),because of the paraxial approximation the configurations in which the polymer folds back onto itself are suppressed; consequently self-avoidance effects are unimportant. The polymer cannot release an imposed twist by passing through itself and so in contrast to the WLC model[23], the free energy is *not* a periodic function of the imposed twist in the PWLC model. We introduce Cartesian coordinates $\xi_1 = \theta\cos\phi$ and $\xi_2 = \theta\sin\phi$ on the tangent plane R^2 at the north pole.

In terms of the Cartesian coordinates we can express the small θ Hamiltonian H as $H = H_P - f$ where H_P is

$$H_P = \frac{1}{2}(p_{\xi_1} - A_{\xi_1})^2 + \frac{1}{2}(p_{\xi_2} - A_{\xi_2})^2 + \frac{f}{2}({\xi_1}^2 + {\xi_2}^2) \tag{2.18}$$

where $A_{\xi_1} = -B\xi_2/2, A_{\xi_2} = B\xi_1/2$. If we have azimuthal symmetry, then the above Hamiltonian becomes-

$$H_P = \frac{1}{2}{p_{\xi_1}}^2 + \frac{1}{2}{p_{\xi_2}}^2 + \frac{(f - \tau^2/4)}{2}({\xi_1}^2 + {\xi_2}^2); \tag{2.19}$$

We immediately notice that H_P is the Hamiltonian of a two-dimensional harmonic oscillator with a frequency $\omega = \sqrt{(f + B^2/4)} = \sqrt{(f - \tau^2/4)}$. For a single oscillator in real time the propagator is given by[20]: $K(\xi_i, \xi_f, T) =$

$$F(T)\exp\frac{i\omega}{2\sin\omega T}[(\xi_i^2 + \xi_f^2)\cos\omega T - 2\xi_i\xi_f] \tag{2.20}$$

where $F(T) = \sqrt{\frac{\omega}{2\pi i\sin(\omega T)}}$.

Setting $\xi_i = \xi_f = 0$ in Eq. (2.20) and continuing the expression to imaginary time we find that the trigonometric functions are replaced by hyperbolic ones. We can express the partition function $Z(f)$ as $\exp(\beta f)$ times the product of the propagators of two independent harmonic oscillators:

$$Z(f,\tau) = \sqrt{f - \tau^2/4}\exp(\beta f)/(2\pi\sinh(\beta\sqrt{f - \tau^2/4})). \tag{2.21}$$

in Euclidean time β.

2.7 Writhe distribution

In this section, we obtain *explicit analytical expressions* the writhe distribution at zero pulling force for the tangent vectors at both the ends of the polymer held fixed. Consider the link distribution-

$$Z(f, Lk) = \int Z(f, B) e^{iBLk} dB \tag{2.22}$$

where we have written $Z(f, B)$ instead of $Z(f, \tau)$. We recall that we have assumed twist to be energetically infinitely expensive and so the applied twist goes completely into writhe; in this limit, the link distribution reduces to the writhe distribution $P(f, W)$. Setting $\alpha = 0$ does not result in any loss of generality; on obtaining the writhe distribution in this limit, the full link distribution $P(f, Lk)$ can be obtained by convolving the writhe distribution with the twist distribution for *all* values of α; in the generating function space, the writhe partition function $Z_W(f, B)$ needs to be multiplied by the factor $\exp(-\alpha B^2/2)$ which pertains to the pure twist distribution at finite α [9, 11]. We shall now derive simple analytical expressions for the writhe distribution.

With the expression for $Z(f, B)$ derived earlier we derive, for $f = 0$, the writhe distribution function as

$$P(f, W) = 1/\cosh(\pi W/\beta)^2 \tag{2.23}$$

The integration in Eqn.(2.23) can be done by going to the complex-B plane and using a semicircular contour closed in the upper-half plane. The integrand has simple poles at $B = i2n\pi/\beta$ at which the residues are evaluated. Finally the sum over residues turns out to be the derivative of a simple geometric series that can be easily evaluated.

Fig.(2.4) shows the plot of the scaled writhe distribution for two different values of β; we notice that for a stiffer polymer, the higher values of writhe are suppressed. This is because for higher rigidity, the bending freedom of the polymer is restricted and high writhe becomes extremely expensive energetically.

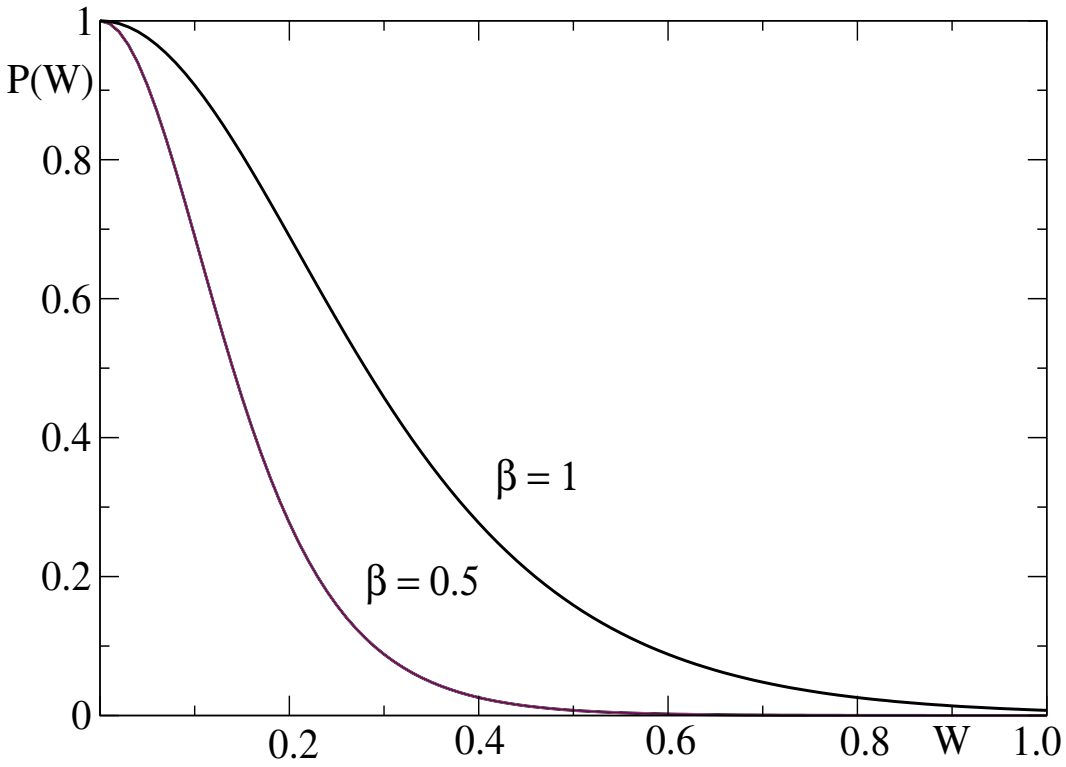

Figure 2.4: The figure shows the writhe distribution for $f = 0$ and $\beta = 0.5, 1$. The tangents at both the ends of the polymer are held fixed. Larger values of the average link (or writhe) are suppressed for the smaller value of β.

2.8 Torque-extension relations

From the expression of the partition function derived before, we calculate the free energy -

$$= \frac{-1}{2\beta} log(f - \tau^2/4) - f + \frac{1}{\beta} log(2\pi) + \frac{1}{\beta} log[\sinh(\beta \sqrt{f - \tau^2/4})] \tag{2.24}$$

The mean extension $< \zeta >=< z > /L = -\partial G(f)/\partial f$ is given by

$$< \zeta >= 1 + 1/(2\beta(f - \tau^2/4) - \coth(\beta \sqrt{f - \tau^2/4})/(2 \sqrt{f - \tau^2/4}). \tag{2.25}$$

where $< \zeta >$ is the $\hat{z}$ component of the extension (or the end-to-end distance vector).

For a stiff polymer even at a zero force, there is a nonzero extension, because of the boundary condition and the stiffness of the polymer. The pure bend model has been studied in Ref[22]; here we study the dependence of the mean extension on the applied torque τ. We find, as expected, that for the a certain applied pulling force, the extension decreases

as the torque is increased. The mean extension is a symmetric function of τ, a feature that is reflected in the symmetry of the *hat curve*. Fig.(2.5) shows that for a constant β, the mean extension is larger for a larger value of the pulling force. In Fig.(2.6), we show the β dependence - the smaller the β (*ie.* the stiffer the polymer), the larger is the extension for the same pulling force. These intuitively clear results follow from our simple analytical

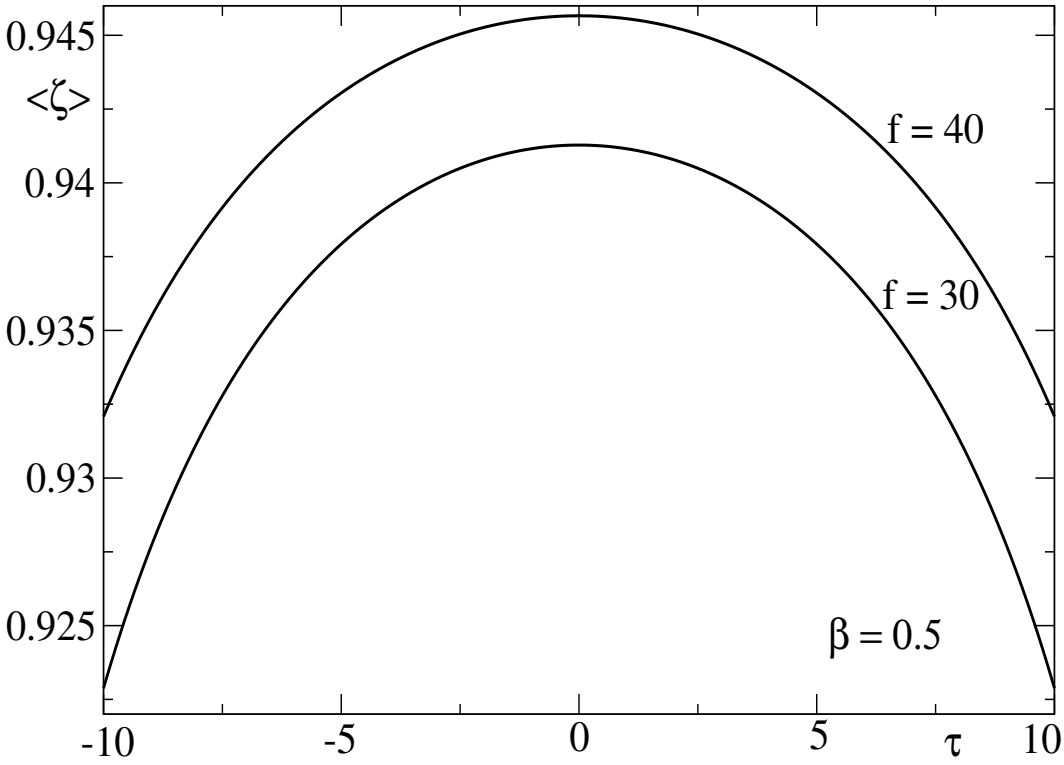

Figure 2.5: The mean extension is plotted against the torque τ for $\beta = 0.5$ and $f = 30, 40$ for a setup with both ends clamped.

2.9 Torque induced buckling

For positive forces, the mean extension increases with increase in force for a fixed value of the torque and decreases with increase of torque when the force is kept fixed. There is a competition between the pulling force and the applied torque. If the force is compressive (negative), the mean extension decreases with increase in the magnitude of the compressive

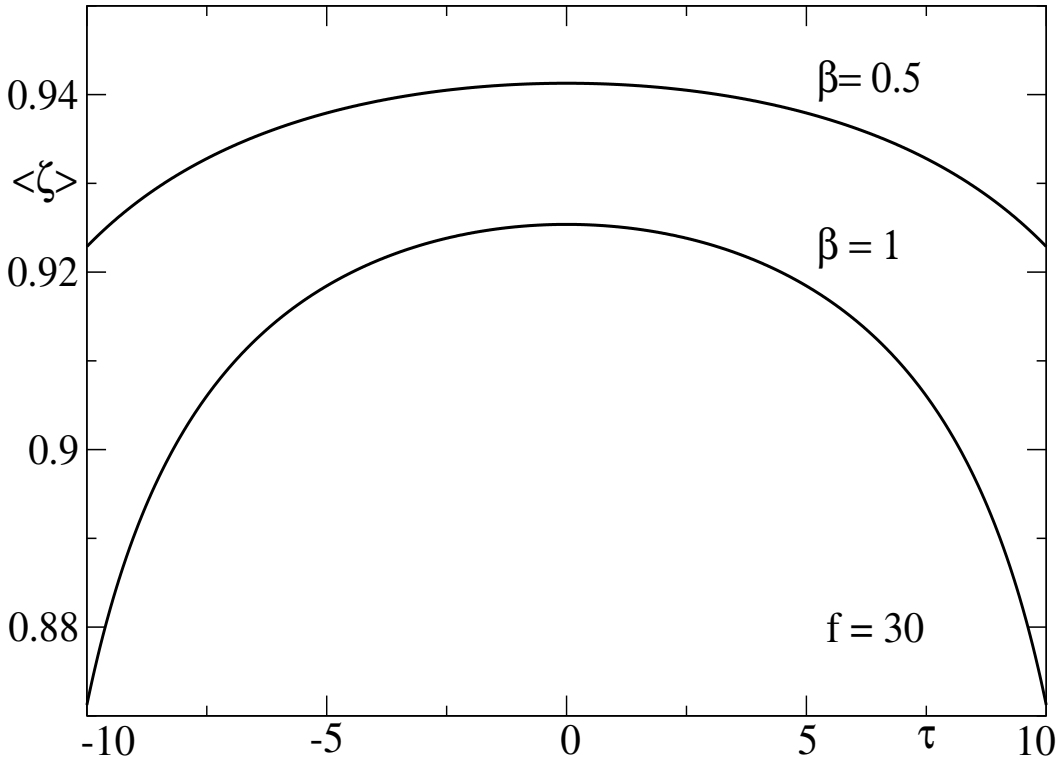

Figure 2.6: The mean extension is plotted as a function of the torque τ for a pulling force $f = 30$ for a stiff polymer with both the ends clamped for $\beta = 0.5$ and $\beta = 1$.

force until at a critical value of the force, the extension sharply decreases[22]; this is a signature of the Euler buckling instability which is seen in thin rods[21]. Let $x = f - \tau^2/4$; for negative x, the hyperbolic functions appearing in Eq.(2.25) go over to circular functions. For instance, when both the end tangent vectors are clamped along the $\hat{z}$ direction, for negative x, the analytical form for the extension becomes

$$< \zeta >= 1 + 1/(2\beta x) - \cot(\beta \sqrt{-x})/(2 \sqrt{-x}). \tag{2.26}$$

which can be rewritten in the form

$$< \zeta >= 1 + \beta u(y). \tag{2.27}$$

where $y = \beta \sqrt{-x}$ and

$$u(y) = \frac{\cot(y)}{2y} - \frac{1}{2y^2}$$

The criterion for the onset of the buckling instability is the divergence of $\partial < \zeta > /\partial\tau$. From Eq.(2.27) this is equivalent to the divergence of $\partial u/\partial y$, which takes place at a value of $y_c = \pi$. This gives us the following expression for the critical torque for buckling at a fixed value of the applied force[21]:

$$(\tau_c/2)^2 = f + (\frac{\pi}{\beta})^2$$

Fig.(2.7) shows a plot of the mean extension vs. the applied torque for the the tangent vectors at both the ends of the polymer fixed. We notice that beyond a certain magnitude of the torque, the extension decreases sharply with very small increase in the torque - this can be interpreted as a signature of buckling instability. From the expression for the critical torque derived above, we see that for $f = 0$, the critical torque $\tau_c = 2\pi/\beta$; the approximate values of the critical torque for $\beta = 0.7$ and $\beta = 0.8$ are 9 and 7.85 respectively. While the $\beta = 0.8$ plot shows distinct signature of buckling at $|\tau| \sim 7.5$, the plot for $\beta = 0.7$ shows no buckling behavior at this range of the value of the torque. As expected, we notice the magnitude of the critical torque τ_c needed to buckle the polymer is larger for a stiffer polymer.

As mentioned before, a stiff polymer is energy dominated and its buckling is very similar to that of a classical rod subject to identical boundary conditions and a compressive force and/or torques. The effect of thermal fluctuations is to slightly smudge the transition point from the straight to the buckled configuration. This is due to thermally activated processes that permit the polymer to overcome the elastic energy barrier. As a result the critical torque for a stiff polymer is slightly smaller in magnitude than the τ_c given above.

2.10 Torque-twist relation

In this section, we present and discuss simple analytical expression for the torque-twist relation. As mentioned earlier, we restrict ourselves to the case of an infinite twist rigidity so that from Fuller's relation $Link = Twist + Writhe$ [25], we see that all of the link resulting from the applied torque goes into the writhe which pertains to the rotation of the axis curve of the polymer in space.

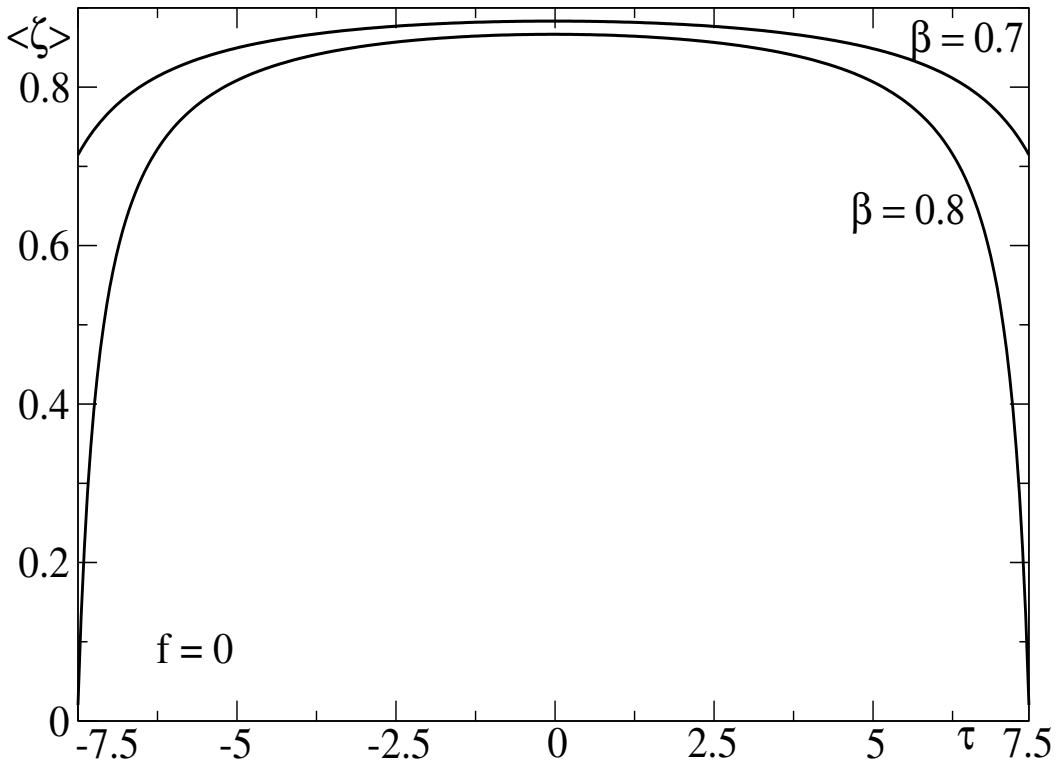

Figure 2.7: The figure shows buckling of the stiff polymer for $f = 0$ and $\beta = 0.7, 0.8$ with the tangent vector at both the ends of the polymer being held fixed.

We differentiate the expression for the free energy wrt the applied torque τ to obtain the torque-twist or, in our case, the torque-writhe relation -

$$< W >= \tau \coth(\beta \sqrt{f - \tau^2/4})/(4 \sqrt{f - \tau^2/4}) - \tau/(4\beta \sqrt{f - \tau^2/4}) \tag{2.28}$$

For the same pulling force, large values of writhe are suppressed for a stiffer polymer (ie. smaller β). Fig.(2.8) shows a plot of the torque-twist relation. From Fig.(2.8) as well as from the analytical expression, we see that the torque-link relation is linear for small applied torques.

2.11 Conclusion

There is a long history of the use of path integrals in the study of polymers [26, 27]. Such methods have been used in the study of elasticity of semiflexible polymers[13, 28, 29, 30]. This connection between path integrals in quantum mechanics and statistical mechanics of

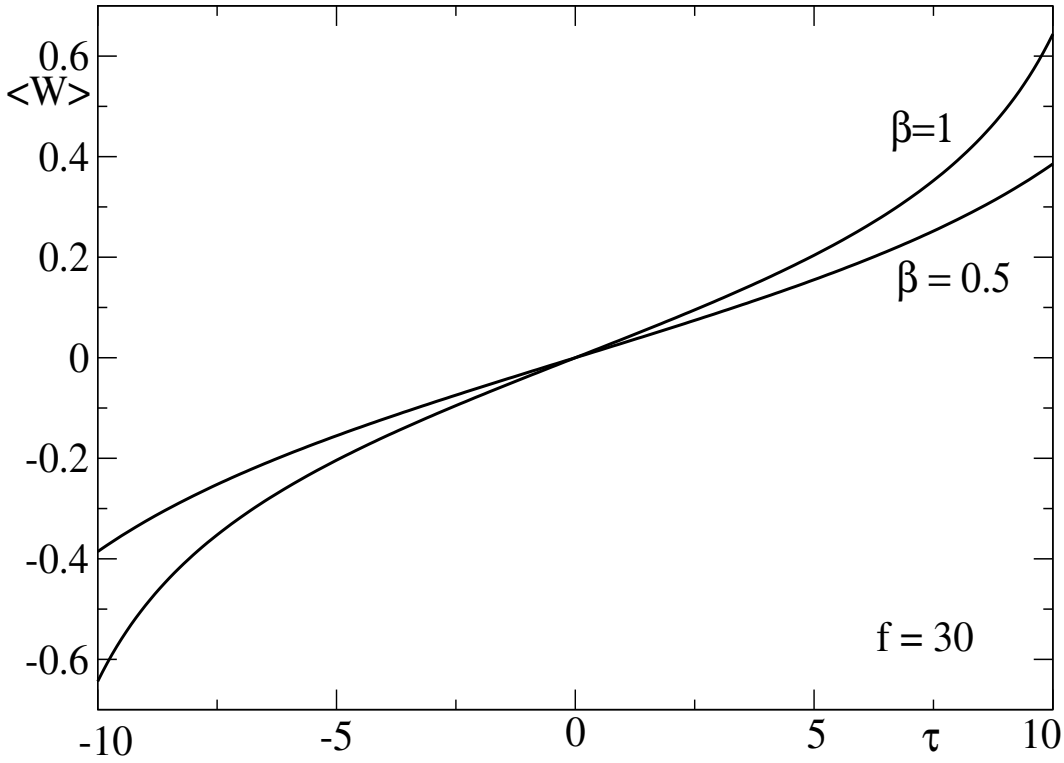

Figure 2.8: The figure shows the torque-link relation for $f = 30$ and $\beta = 0.5, 1$. For the same applied torque, larger values of the average link (or writhe) are suppressed for the stiffer polymer.

polymers enables us to import ideas back and forth between these two distinct domains. It is quite interesting that standard results in path integrals give us new results for stiff biopolymers. In this chapter we have theoretically studied the elasticity of stiff biopolymers. We have studied some cases with boundary conditions realizable in single molecule experiments. By attaching a magnetic bead to an end of the polymer, one can apply forces using magnetic field gradients and torques using magnetic fields. By such techniques one can impose a variety of boundary conditions on the polymer including the ones discussed here. Recent studies have shown [2] that the elastic behavior of such a biopolymer at the single molecular level affects the elastic properties of a biopolymer network. In a cytoskeletal structure the end tangent vectors of the stiff biopolymers that make up the structure are pinned. A cytoskeleton can be viewed as a replica of a large number N of semiflexible polymers. By studying the elastic properties of a single polymer constituting such a network, we can draw conclu-

sions regarding the stability of the N polymer cytoskeletal structure. Here we have presented closed form simple analytical expressions for force-extension relations for a single stiff filament which can be tested against single molecule experiments. These analytical results are new and are expected to shed light on the structural stability of the N polymer cytoskeletal structure. An understanding of the bending and torsional elastic properties of actin is vitally important for understanding biological phenomena like muscle contraction, motion of motor proteins and the role of the cytoskeleton in determining the shape of the cell [31].

We have also considered the case in which one end of a stiff polymer is clamped and the other end is free. This is a boundary condition that is more natural to an experimental setup for measuring the end-to-end distance distribution $P(\zeta)$ of a polymer via imaging of a polymer tagged with fluorescent dye. In fact one can construct a force-extension curve from the experimental data of $P(\zeta)$ versus ζ. We have theoretically analyzed this case and made predictions for experiments in this case as well. As in the earlier case, in this case also we have a simple analytic form. In the context of studying twist elasticity, this boundary condition is untenable because the molecule can release link and relax by the process of "geometric untwisting"[32]. We have derived an analytical expression for the writhe distribution for zero pulling forces. The writhe distribution has important implications in the context of transcription and gene regulation. Knowledge of writhing of a biopolymer backbone and it's stabilization is crucial for understanding the cellular processes mentioned above. We have also derived simple expressions for the torque-link relation.

In future it would be interesting to study the buckling of stiff filaments like actin in greater detail. This is an issue that is of relevance at the single molecular level as well as at the level of a biopolymer network like the cytoskeletal structure and is expected to shed light on its structural stability[2, 33] and collapse under stress. The stiffness and collapse of the cytoskeletal structure of a red blood cell[33] has a direct connection to its functional aspects and used for instance, as a diagnostic for detection of sickle cell anaemia. In studying the cytoskeletal structure it would be most useful to have a good understanding of the individual polymers that make up the structure. Simple analytic forms give valuable insight into a

problem and we expect the analytic results presented here to provide some fresh impetus to this rapidly growing field of semiflexible polymers.

Bibliography

[1] B. Alberts et al, *Molecular Biology Of The Cell* (Garland Publishing, New York, 1994), 3rd ed.

[2] P. Fernandez et al, Biophysical Journal **90**, 1 (2006) and references therein.

[3] P. Nelson, Biological Physics: Energy, Information, Life, (W. H. Freeman, 2003).

[4] Z. Dogic et al, *Phys. Rev. Lett.* **92**, 125503 (2004).

[5] C. Bustamante et al, Current Opinion in Structural Biology **10**, 279 (2000).

[6] A. Ott, M. Magnasco, A. Simon and A. Libchaber, *Phys. Rev.* **E48**, R1642 (1993).

[7] L. Le Goff, O. Hallatschek, E. Frey and F. Amblard, *Phys. Rev. Lett.* **89**, 258101 (2002)

[8] O. Kratky and G. Porod, *Rec. Trav. Chim. Pays-Bas.* **68** 1106-1123 (1949).

[9] C. Bouchiat and M.Mezard, *Phys. Rev. Lett.* **80**, 1556 (1998)

[10] Moroz J D and Nelson P, *Proc. Natl. Acad. Sci. USA* **94**, 14418 (1997).

[11] S. Sinha, *Physical Review E* **70** 011801 (2004).

[12] J. Samuel, S. Sinha and A. Ghosh *Journal of Physics: Condensed Matter*, **18** S253 (2006).

[13] J. Samuel and S. Sinha, *Physical Review E*, **66** 050801(R) (2002); S. Stepanow and G. M. Schütz, *Europhysics Letters*, **60** 546 (2002).

[14] S. Sinha and J. Samuel, *Physical Review E* **71**, 021104 (2005).

[15] A. Dhar and D. Chaudhuri, *Phys. Rev. Lett.* **89**, 065502 (2002).

[16] H. J. Kreuzer and S. H. Payne, *Phys. Rev.* **E 63**,021906 (2001).

[17] P. Ranjith, P.B. Sunil Kumar and G.I. Menon, *Physical Review Letters*, **94** 138102 (2005).

[18] J. Marko and E. D. Siggia, Macromolecules **28**, 8759 (1995).

[19] Stephen Wolfram, The Mathematica Book, Third Edition (Wolfram Media/ Cambridge University Press,1996).

[20] R. P. Feynman and A. R. Hibbs, Quantum Mechanics and Path Integrals, (McGraw-Hill Companies, 1965).

[21] L. D. Landau and E. M. Lifshitz, Theory of Elasticity, pg 98, Problem 2 (Pergamon Press Ltd. (1970) Britain.

[22] Abhijit Ghosh, Joseph Samuel and Supurna Sinha, *Phys. Rev. E* **76**, 1 (2007)

[23] J. Samuel and S. Sinha, *Phys. Rev. Lett.* **90**, 098305 (2003)

[24] J.Wilhelm and E.Frey, *Phys. Rev. Lett.* **77**, 2581 (1996)

[25] F B Fuller *PNAS* **68** 815 (1971), PNAS **75** 3557 (1978)

[26] L.S. Schulman, Techniques and Applications of Path Integration, (Wiley Interscience,1981)

[27] S. F. Edwards and M. Doi, The Theory of Polymer Dynamics, (Oxford University Press, Oxford, 1986).

[28] H. Kleinert, Path Integrals in Quantum Mechanics, Statistics, Polymer Physics and Financial Markets, (World scientific, Singapore, 2006, 4. ed.)

[29] N. Saito, K. Takahashi and Y. Yunoki *J. Phys. Soc. Jpn* **22**, 219 (1967).

[30] H. Yamakawa, Helical Wormlike Chains in Polymer Solutions, (Springer, New York, 1997).

[31] Yuri Tsuda et al, *PNAS* **93** 12937-12942 (1996)

[32] R. E. Goldstein et al, *Phys. Rev. Lett.* **80**, 5232 (1998)

[33] A. Ghosh et al, *Phys. Biol.* **3** 67-73 (2006).